Computer Assisted Mechanics and Engineering Sciences, 6: 217–229, 1999.

Chaotic oscillations in a model of suspended elastic cable under planar excitation

Wanda Szemplińska-Stupnicka, Elżbieta Tyrkiel, Andrzej Zubrzycki
Institute of Fundamental Technological Research, Polish Academy of Sciences
ul. Świętokrzyska 21, 00-049 Warszawa, Poland

(Received August 17, 1998)

The single mode equation of motion of a suspended elastic cable under planar excitation is considered, and numerical exploration is focused on the chaotic oscillations which occur in a certain domain of system control parameters. Bifurcations of the subharmonic resonance oscillation and their evolution into chaotic attractor are studied. Then the global bifurcation theory is applied to determine the critical system parameters for which the chaotic attractor undergoes the subduction destruction in the "boundary crisis" scenario. The post-crisis transient motion, which in this case becomes the generic long-lasting chaotic system response, is also studied.

1. Introduction

The nonlinear planar oscillations of a suspended elastic cable were studied extensively in a series of papers by Rega and his associates [1, 2, 11, 12]. An essential progress in the investigation of strongly nonlinear and chaotic phenomena was due to the reduction of the original partial integro-differential equation of motion to a single-mode motion mathematical model. This model made it possible to apply the theory of bifurcation and the methods developed recently for chaotic dynamical systems [6, 10, 20]. The mathematical model takes the form of the second order ordinary differential equation with a forcing term. The main features of the relevant dynamical problems are associated with the presence of both quadratic and cubic nonlinearity in the equation of motion.

In this type of dynamical system the chaotic attractor was found for the first time by Ueda [19] with the aid of analog computer. Further studies revealed that various interesting bifurcational phenomena were closely related to the 2T-periodic resonance, and that the concept of stability limit of the periodic solutions of different periods plays an essential role in understanding the occurrence of the chaotic oscillations. Due to this observation some relations between various periodic solutions studied by the approximate analytical methods and the chaotic solution obtained by computer-based method were established [14, 16, 17].

In the earlier literature an attention was focused on the evolution of the periodic subharmonic solution into chaotic motion, i.e. on the bifurcation and explosion of the chaotic attractor. Little attention was paid to the mechanism of destruction of the chaotic attractor (crisis), its disappearance from the phase space and the further post-crisis system response.

The goal of this paper is twofold:

1. First we try to explore the bifurcation of the system response taking into account both branches of the subharmonic resonance — the nonresonant and the resonant isolated solution branch. In the earlier literature bifurcation of only the nonresonant branch was studied, the branch which evolves from the nonresonant T-periodic solution. The first period-doubling bifurcation of the solution gives rise to the nonresonant branch of the 2T-periodic subharmonic resonance, and the further series of bifurcations (observed at decreasing the driving frequency) leads to the generation of the chaotic attractor. But the theory and computer simulation reveal an existence

(and coexistence) also of the isolated, resonant branch of the subharmonic resonance solution. In the paper we try to explore the sequence of bifurcations that occur at the resonant branch, and to establish a relation between the chaotic attractor that evolves from the nonresonant T-periodic solution and the chaotic one, which, possibly, evolves from the resonant branch of the 2T-periodic subharmonic resonance.

2. Then we investigate the mechanism of destruction of the chaotic attractor by the use of the global bifurcation theory. We show that the destruction is due to the "boundary crisis" of the chaotic attractor, the phenomenon which originally was defined as "a collision of the chaotic attractor with an unstable orbit not on the attractor" [4, 5]. Further studies revealed that the phenomena can be also defined in terms of the global bifurcation theory. First, it was proved that the boundary crisis is also defined by the homoclinic bifurcation of the unstable orbit not on the attractor, the orbit whose stable invariant manifolds form a boundary of the basin of attraction of the chaotic attractor. In the paper we verify by numerical computation another theoretical approach to the boundary crisis. We show that the boundary crisis can be also defined as the heteroclinic bifurcation of the unstable orbit not on the attractor and the principal saddle of the chaotic attractor [8].

We also want to draw an attention on the post-crisis response of the system — the response that belongs to the category of the long-lasting, unpredictable chaotic transient. This class of motion was already studied by the Authors in association with the occurrence of fractal basin boundaries of coexisting periodic attractors [18]. In this paper we show and illustrate the other case, when the chaotic transient motion becomes a generic response of the system.

In Section 2 we begin with a review of the derivation of the single-mode equation of motion of a suspended elastic cable, and of the approximate analytical results (amplitude–frequency characteristics) of the T-periodic (primary resonance) and 2T-periodic (subharmonic resonance) solutions, as well as of the early analog-computer results indicating occurrence of chaotic oscillations. Although in recent publications additional chaotic motions zones were found which appeared to be related to the 3T-periodic subharmonic resonance, only that one which occurs close to the stability limit of the 2T-periodic resonance occupies a significant region in the system control parameter plane and is considered in the present paper [12]. In Section 3 we discuss our main results concerning the bifurcation diagram of the both (resonant and nonresonant) branches of the 2T-periodic subharmonic resonance, the theoretical aspects of the boundary crisis of the chaotic attractor, and the post-crisis chaotic transient motion.

2. Equation of the single-mode motion of a suspended elastic cable and the approximate analytical study

We consider a heavy elastic cable suspended between two fixed supports at the same level (Fig. 1). The single-mode motion of the system subject to planar excitation was derived by Benedettini and Rega [1]. The initial state equilibrium configuration C^1, which is assumed as a referenced configuration in the zy plane, is represented by a parametric function $y(s)$, s being a curvilinear abscissa. The varied configuration C^ν occupied by the cable under action of a vertical distributed load $p(s,t)$ is described by the horizontal and vertical displacement coordinates $u(s,t)$, $v(s,t)$ of a point $P(s)$.

The equations of motion of the cable are obtained by the use of the extended Hamilton's principle (for details we refer the reader to [1]). The following assumptions are made:

(i) the static equilibrium configuration of the cable is described through parabola

$$y = 4d\left\{\frac{z}{l} - \left(\frac{z}{l}\right)^2\right\},$$

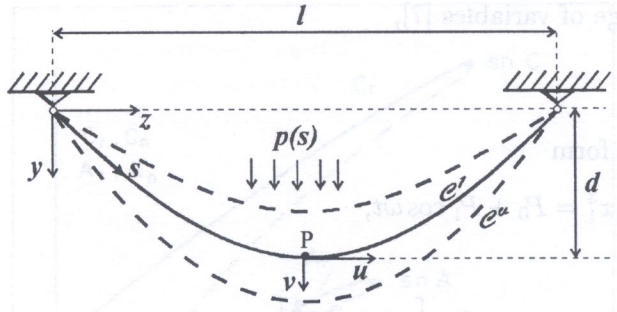

Fig. 1. Static and dynamic cable configurations

which entails $d_s \simeq d_z$ and $T^l \simeq H$, H standing for the horizontal component of the initial tension, T^l — for the cable tension in the initial configuration;

(ii) the gradient of the horizontal component of the dynamic displacement is negligible with respect to unity, i.e. moderately large rotations occur in the cable motion;

(iii) the longitudinal inertia forces $m\ddot{u}$ are neglected.

Under these assumptions the cable motion can be described by the unique partial integro-differential equation in the vertical displacement $v(s,t)$

$$m\ddot{v} - \left\{ H\dot{v} + \left[\frac{EA}{l}\right](y' + v') \int_0^l \left[y'v' + \frac{(v')^2}{2} \right] dz \right\}' + \delta\dot{v} = p(s,t) \tag{1}$$

where the prime states for $\partial/\partial z$ and the dot — for $\partial/\partial t$; E, A and m denote the elastic modulus, the cross sectional area and the mass per unit length, respectively, and δ is a viscous damping coefficient per unit length.

Equation (1) is accurate for studying suspended cables used in overhead transmission lines for which the sag-to-span ratio $d/l \cong 1/20$, $H/EA = O[(d/l)^2]$, and the dynamical displacement components are, respectively, $u = O(\varepsilon d^2/l)$ and $v = O(\varepsilon d)$, with ε being a small parameter of the order of amplitude.

A nondimensional form of the equation of motion is obtained by introducing the following normalized variables:

$$\tilde{z} = \frac{z}{l}, \qquad \tilde{v} = \frac{v}{d}, \qquad \tilde{t} = \omega_0 t, \qquad \tilde{\delta} = \frac{\delta\omega_0 l^2}{H}, \qquad \tilde{p} = \frac{pl^2}{Hd}, \tag{2}$$

where ω_0 is the natural frequency of the linearized system (1). For the sake of simplicity, the sign of tilde will be omitted in the subsequent expressions.

By representing the displacement through the eigenfunction $\Psi(z)$ corresponding to the frequency ω_0, and a time function $x(t)$, and by considering a monofrequent harmonic excitation of frequency ω with the given spatial distribution $\Phi(z)$,

$$v(z,t) = \Psi(z)x(t), \qquad p(z,t) = \Phi(z)P\cos\omega t, \tag{3}$$

one can apply the conventional Galerkin projection method and arrive at the following single ordinary differential equation of motion in the variable x,

$$\ddot{x} + h\dot{x} + \Omega_0^2 x + \alpha_2 x^2 + \alpha_3 x^3 = F\cos\omega t, \qquad \alpha_3 > 0; \tag{4}$$

where the coefficients h, Ω_0^2, α_2, α_3, F are uniquely determined by the parameters of Eqs. (1), (3) and the shape functions $\Psi(z)$, $\Phi(z)$.

By applying the change of variables [7],

$$x_1 = x + \frac{\alpha_2}{3\alpha_3}, \tag{5}$$

Eq. (4) is reduced to the form

$$\ddot{x}_1 + h\dot{x}_1 + C_1^2 x_1 + \alpha_3 x_1^3 = P_0 + P_1 \cos \omega t, \tag{6}$$

where

$$C_1^2 = \Omega_0^2 - \frac{1}{3}\frac{\alpha_2^2}{\alpha_3}, \qquad P_0 = \frac{\alpha_2}{3\alpha_3}\left[\Omega_0^2 - \frac{2}{9}\frac{\alpha_2^2}{\alpha_3}\right], \qquad P_1 \equiv F. \tag{7}$$

Equation of the single-mode motion of the elastic cable in the form (4) is suitable for our numerical analysis; the transformed equation (6) enables us to relate the present results to those obtained earlier by the use of analog computer and the approximate analytical methods [14, 17, 19].

The potential energy $V(x)$ of the system governed by Eq. (4),

$$V(x) = \frac{1}{2}\Omega_0^2 x^2 + \frac{1}{3}\alpha_2 x^3 + \frac{1}{4}\alpha_3 x^4,$$

possesses single equilibrium position x_e at $F = 0$,

$$x_e = 0,$$

which is stable:

$$\left.\frac{d^2V}{dx^2}\right|_{x=0} = \Omega_0^2 > 0.$$

The corresponding equilibrium position of the system governed by Eq. (6) is biased due to the action of the constant force P_0. For instance, at $P_1 = 0$, $P_0 \neq 0$ and $C_1^2 = 0$, the equilibrium position is given by

$$x_{1e} = \sqrt[3]{P_0}.$$

In this case, by the successive change of variables,

$$x_2 = x_1 + \sqrt[3]{P_0},$$

Eq. (6) can be reduced to the form

$$\ddot{x}_2 + h\dot{x}_2 + x_2^3 = P_0 + P_1 \cos \omega t. \tag{8}$$

One can also arrive at Eq. (8) from Eq. (4) under the following assumptions [17]:

$$\Omega_0^2 = \sqrt[3]{P_0^2}; \qquad \alpha_2 = \sqrt[3]{P_0}; \qquad \alpha_3 = 1, \qquad x_2 = x + \sqrt[3]{P_0}.$$

The first reports on the occurrence of chaotic oscillations in the system governed by Eq. (8) is due to Ueda, 1980 [19]. By the use of analog computer he investigated the system response at three different values of the parameter P_0 ($P_0 = 0.020$; $P_0 = 0.030$; $P_0 = 0.045$), with the other coefficients kept constant: $P_1 = 0.16$, $h = 0.05$, and showed that in certain region of the control parameters of the system the periodic oscillation evolves into aperiodic and unpredictable chaotic response.

Further investigations based on the approximate analytical methods combined with the analog computer study brought the observation that the zone of chaotic motion is related to the stability limit of the 2T-periodic subharmonic resonance, i.e. chaos occurs in the neighborhood of the critical system parameters for which, in weakly nonlinear system, the 2T-periodic solution loses stability

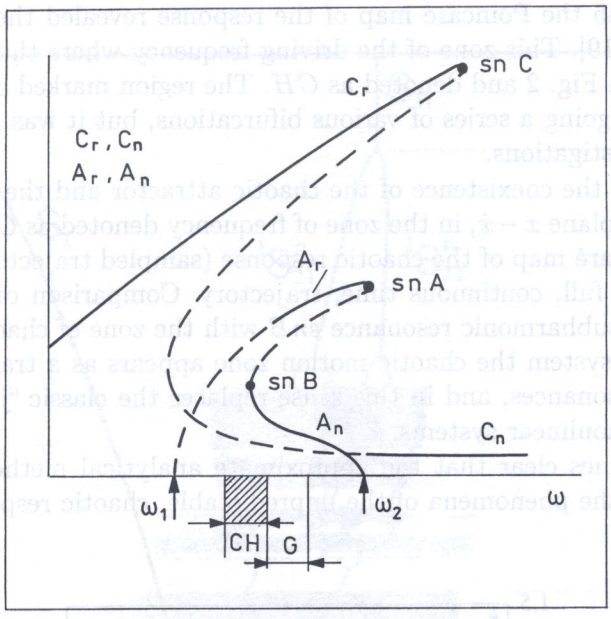

Fig. 2. Schematic diagram of the amplitude–frequency curves of the approximate periodic solutions in the region of the 1/2 subharmonic resonance

in favor of the primary resonant T-periodic solution. In this section we recall and review these problems, because the analysis of periodic solutions appeared to be an essential step in the further development of knowledge and understanding of the phenomena of chaotic oscillations in the single-well potential, dissipative nonlinear oscillator driven by periodic force.

Our present analysis relates to the system governed by Eq. (8) with the coefficients of Ueda [19], i.e.: $h = 0.05$, $C_1^2 = 0$, $\alpha_3 = 1$, $P_1 = 0.16$, $P_0 = 0.045$. The equivalent coefficients in Eq. (4) are: $h = 0.05$, $\Omega_0^2 = 0.38$, $\alpha_2 = 1.067$, $\alpha_3 = 1$, $P_1 = 0.16$.

We begin with the schematic diagram of the amplitude–frequency curves of the approximate periodic solutions, shown in Fig. 2. For the primary, T-periodic resonance the first approximate solution is assumed in the form

$$x_s(t) = x_s(t+T) = C_0 + C\sin(\omega t + \varphi_1), \tag{9}$$

and for the subharmonic, 2T-periodic resonance the solution is put as

$$x_s(t) = x_s(t+2T) = C_0 + C\cos(\omega t + \varphi_1) + A\sin(\frac{\omega}{2}t + \varphi_2), \tag{10}$$

where the amplitudes A, C_0 , C and the phase angles φ_1, φ_2 are determined by the harmonic balance method [7, 15]. The dashed branches of the amplitude–frequency curves $C \equiv C(\omega)$, $A \equiv A(\omega)$ denote unstable solutions (saddles). Points of vertical tangents snA, snB, snC correspond to the stability limits, or, in terminology of the bifurcation theory, to the saddle-node bifurcations. Due to the nonlinear term in the equation of motion (6) the resonance curves exhibit "nonlinear resonance hysteresis", i.e. at certain zone of the driving frequency ω two stable solutions — the resonant and nonresonant ones — coexist; they are denoted as A_r , C_r and A_n , C_n , respectively.

It was found that at the low values of the coefficient P_0, e.g. $P_0 = 0.20$, the system response examined by analog computer was very close to that assumed by the first approximate solutions, given by Eqs. (9), (10). If the computer simulation was started at $\omega > \omega_2$ at zero initial conditions and the driving frequency was gradually decreased, the system exhibited first the nonresonant low amplitude primary resonance solution C_n and then, at $\omega = \omega_2$ the subharmonic term A_n appeared, so that the T-periodic solution bifurcated into the 2T-periodic resonance. At the stability limit snB the system exhibited jump to the high amplitude primary resonant solution C_r . The isolated branch of the subharmonic resonance curve (A_r in Fig. 2) was not considered in that time.

At the value $P_0 = 0.45$ the Poincaré map of the response revealed the existence of the strange attractor in the system [19]. This zone of the driving frequency where the chaotic motion occurs is schematically depicted in Fig. 2 and denoted as CH. The region marked as G indicates the zone of irregular response, undergoing a series of various bifurcations, but it was not recognized as "chaos" in the early stage of investigations.

In Fig. 3 we illustrate the coexistence of the chaotic attractor and the T-periodic primary resonance orbit in the phase plane $x - \dot{x}$, in the zone of frequency denoted as CH. The chaotic attractor is represented by a Poincaré map of the chaotic response (sampled trajectory), while the T-periodic solution is shown as the full, continuous time, trajectory. Comparison of the theoretical stability limit of the 2T-periodic subharmonic resonance snB with the zone of chaotic motion shows that in the single-well potential system the chaotic motion zone appears as a transition zone between the two different periodic resonances, and in this sense replaces the classic "jump phenomena" known in the theory of weakly nonlinear systems.

At this point it becomes clear that the approximate analytical methods can not be useful to explain and understand the phenomena of the unpredictable, chaotic response in this region of the system parameters.

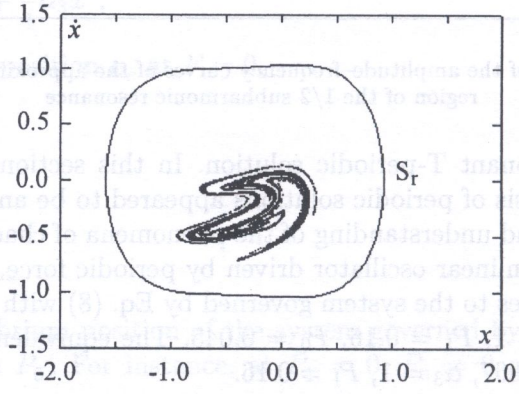

Fig. 3. Coexistence of the resonant T-periodic attractor (continuous time trajectory) and the chaotic attractor (sampled trajectory); $\omega = 1.0$

3. Evolution of the 2T-periodic subharmonic resonance into chaotic attractor, the boundary crisis, and the post-crisis transient response

The results obtained and presented in this section are based on numerical analysis of the response of the nonlinear oscillator, governed by Eq. (4). The *Dynamics* computer program [9] proved to be very useful in our investigations.

To get an insight into the behavior of the system at the subharmonic resonance region and all these bifurcations that turn the 2T-periodic solution into the chaotic motion, we apply the concept of maps and examine the bifurcation diagram for both branches of the subharmonic resonance: the nonresonant one (denoted as S^n_{2T}), which bifurcates from the T-periodic solution (denoted as S_n), and the resonant 2T-periodic isolated solution (denoted as S^r_{2T}). In the bifurcation diagram the sampled T-periodic response $x(nT)$, $n = 0, 1, 2, \ldots$, is represented by a single line (drawn versus the driving frequency), and the 2T-periodic response — by two lines. Chaotic response is represented by, theoretically, infinite number of points at $\omega = \text{const}$, but in the computer realization — by a large number of points, and it looks like a shaded region (Figs. 4a,b,c).

Figure 4a shows the sequence of bifurcations of the solution, which for $\omega > \omega_2$ is T-periodic, and represents the nonresonant branch of the primary resonance S_n (see Fig. 2). With the decrease of the driving frequency ω, at $\omega_{pd} \approx 1.37$ the T-periodic solution S_n loses its stability and undergoes the period-doubling bifurcation; the post-bifurcation stable solution S^n_{2T} is denoted by two points

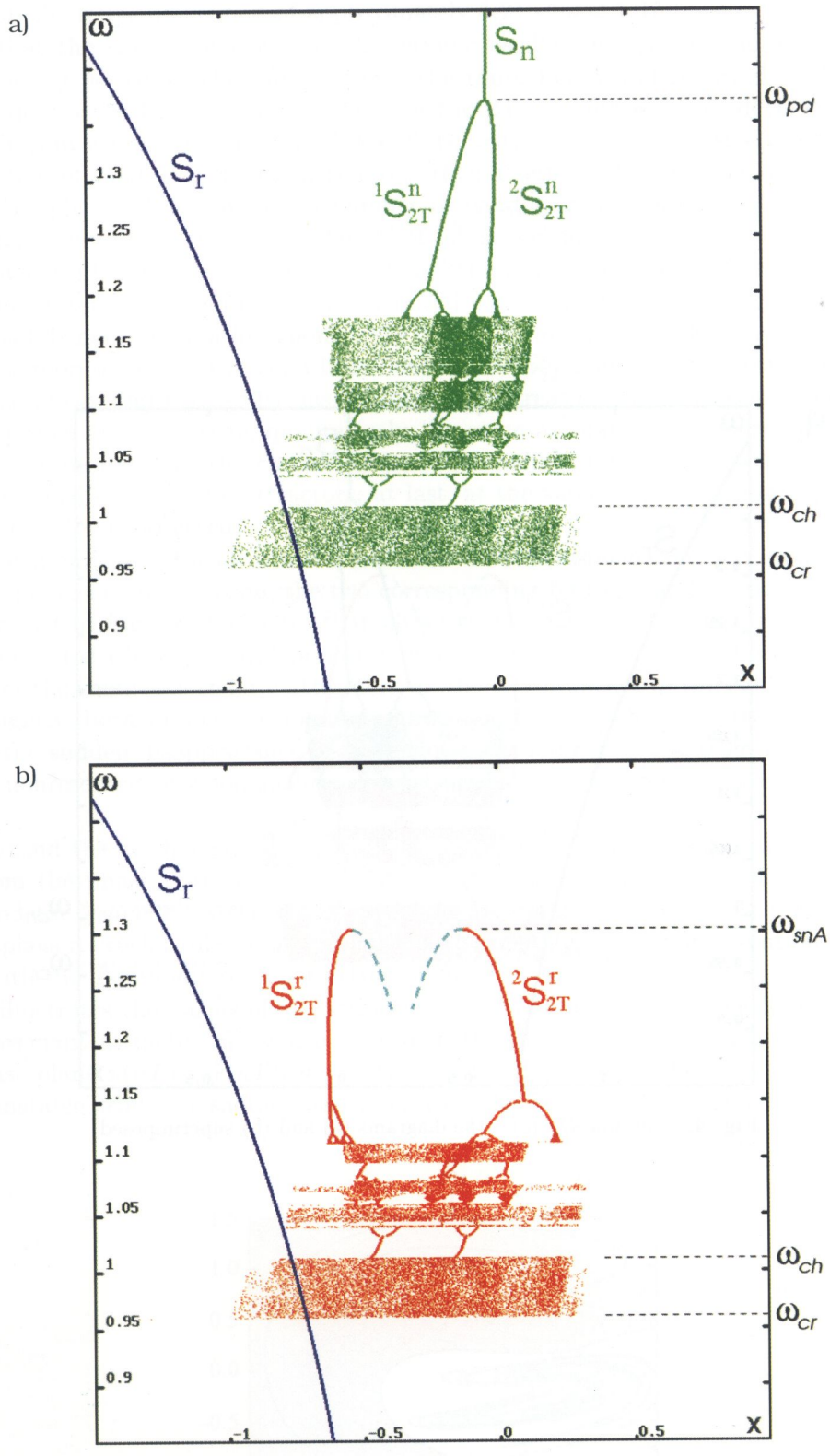

Fig. 4. Bifurcation diagrams of the subharmonic resonance solutions S^n_{2T}, S^r_{2T} with decreasing the driving frequency ω; the coexisting T-periodic resonance solution S_r is also depicted: (a) the nonresonant branch S^n_{2T}; (b) the resonant branch S^r_{2T}; *(continued in the next page)*

c)

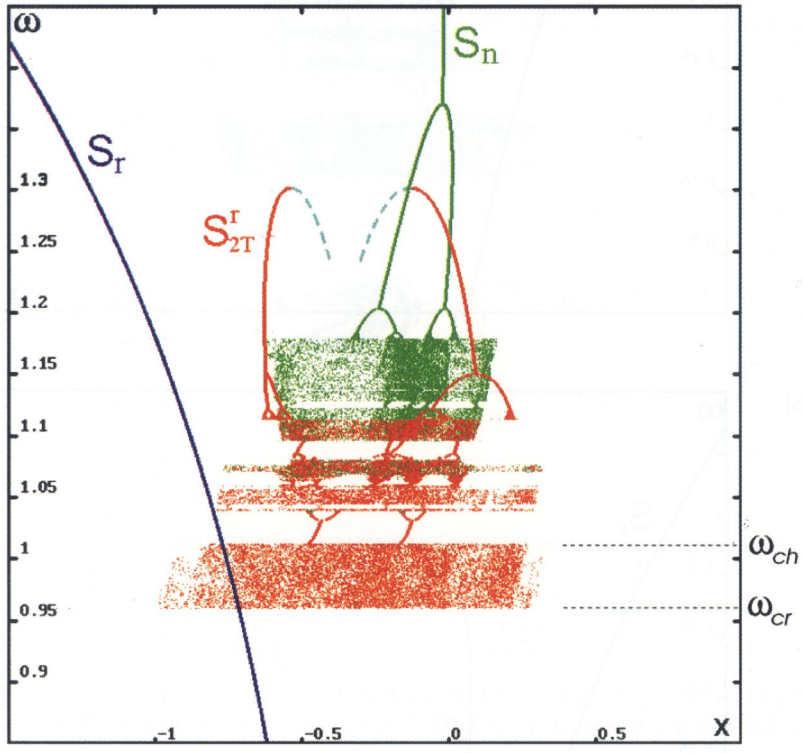

Fig. 4. *(continued)*; (c) – the diagrams (a) and (b) superimposed

${}^1S^n_{2T}$ and ${}^2S^n_{2T}$, and it represents the nonresonant branch of the 2T-periodic subharmonic resonance which exists in the frequency region of approximately $1.21 < \omega < 1.37$.

We note that the transition from the 2T-periodic oscillation S^n_{2T} to chaotic motion develops via the *cascade of period-doubling bifurcations*, the route found and reported by Feigenbaum in 1978 [3]. At decreasing the driving frequency ω the 2T-periodic solution develops the series of period-doublings in which orbits of period 2×2^n $(n = 1, 2, \ldots)$ are successively produced, leading to the generation of small-size chaotic attractors; then a series of bifurcations of small-size chaotic attractors takes place, which involves a number of band mergings alternately with a number of periodic windows; finally, at $\omega = \omega_{ch}$, a "burst" of full size chaotic attractor appears.

Let us now consider the resonant branch of the 2T-periodic resonance. The isolated solution is realized in the system under properly chosen initial conditions (or disturbance of motion) and is born in the saddle-node bifurcation (point snA in Fig. 2) at $\omega_{snA} \approx 1.30$. The stable 2T-periodic solution S^r_{2T} is represented by two solid lines denoted as ${}^1S^r_{2T}$ and ${}^2S^r_{2T}$. A portion of the unstable solution is also drawn and marked by dashed lines. At decreasing the driving frequency ω we again observe a sequence of bifurcations qualitatively the same as that of the nonresonant branch: the 2T-periodic solution develops the cascade of period-doublings followed by a series of bifurcations (explosions) of small-size chaotic attractors; at last, at the value $\omega_{ch} \approx 1.07$, an explosion of a full size chaotic attractor is observed.

To a clear comparison of the bifurcation scenarios of both (resonant and nonresonant) branches of the subharmonic resonance solution, the two corresponding bifurcation diagrams (Figs. 4a and 4b) are superimposed in Fig. 4c. We note, that although there is a difference between the values of the parameter ω for which the first period-doubling of the 2T-periodic solution occurs, and the bifurcations of the small-size chaotic attractors on the two branches of the subharmonic resonance also differ slightly, both branches evolve into the same full size chaotic attractor at $\omega = \omega_{ch}$. It follows that the sudden disappearance of the chaotic attractor at $\omega_{cr} \approx 0.96$ occurs in the system whether the nonresonant or resonant branch of the subharmonic resonance is realized prior to the crisis.

To understand the mechanism of the sudden loss of stability and disappearance of the chaotic attractor from the phase portrait we make use of the concept of maps applied to the *basins of attraction* and the *geometric structure of invariant manifolds* of an unstable orbit. The unstable orbit which plays a crucial role in the problem is the unstable T-periodic solution (cyclic saddle) associated with the T-periodic resonant attractor S_r.

Figure 5 illustrates the basins of attraction of the two attractors: the chaotic attractor and the T-periodic resonant attractor S_r, which coexist in the zone of frequency $\omega_{cr} < \omega < \omega_{ch}$. In the sampled phase plane $x(nT) - \dot{x}(nT)$, $n = 0, 1, 2, \ldots$, the T-periodic orbits are represented by fixed points; the unstable orbit (the saddle) associated with the T-periodic attractor S_r is denoted as D_r.

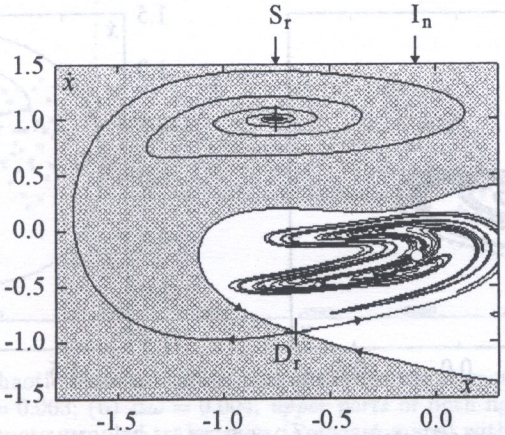

Fig. 5. Basins of attraction of the T-periodic attractor S_r (grey) and the chaotic attractor (white); $\omega = 1.0$

The invariant manifolds of the saddles are mapped here as smooth lines: the unstable manifold (left outset) tends to the periodic attractor S_r and the other branch (right outset) forms a complicated structure. From the recent publications [4, 8] it is known that, in fact, the structure of this outset is very close to the structure of the chaotic attractor. The two stable manifolds of D_r (insets) define the boundary of the basins of attraction of the two coexisting attractors: S_r and the chaotic attractor.

Now let us look at the following problem: what happens if at further decrease of ω the insets of D_r and the right hand side outset of D_r became tangent and next, begin to intersect? Thus we came to the concept of the *homoclinic bifurcation*. At this point it is essential to notice, that, if the two invariant manifolds intersect once, they will intersect infinitely many times. The consequence of the bifurcation is the catastrophe for the chaotic attractor: its basin of attraction and the attractor itself cease to exist [13].

Recently another interpretation of the boundary crisis in the light of the global bifurcation theory is considered. It is based on the theoretical conclusion that the two different geometric structures: the outset of D_r which tends to the chaotic attractor (the right-hand branch in Fig. 5) and the outset of the principal saddle of the chaotic attractor (i.e. the inverse saddle I_n in our example) are extremely close to each other in the phase space [5, 8]. This implies that the boundary crisis can be defined either by the homoclinic bifurcation of D_r or by the heteroclinic bifurcation of D_r and I_n. In other words, the two types of global bifurcations should occur at the same (in the sense of the accuracy of numerical computation) values of the control parameters. The equivalence of the three definitions of the boundary crisis can be verified only by "numerical evidence". In the paper we computed the critical values of the boundary crisis of the chaotic attractor by making use of all the three criteria: (i) boundary crisis as a collision of the chaotic attractor with the saddle D_r; (ii) boundary crisis as the homoclinic bifurcation of the saddle D_r; (iii) boundary crisis as the heteroclinic bifurcation of the saddle D_r and the inverse saddle I_n . Numerical computation confirms that indeed the three types of bifurcations occur at the same values of the system parameters and, therefore, each of them can be used as a criterion of the boundary crisis. The results are presented in Figs. 6a and 6b. In Fig. 6a the collision of the chaotic attractor (represented by a Poincaré map of the chaotic trajectory) and the saddle D_r is illustrated. Then the heteroclinic bifurcation as defined by the tangency condition of the right-hand outset of D_r and the inset of I_n is shown. The homoclinic bifurcation of D_r is not presented on a separate figure, because, in fact, the geometrical structure of the invariant manifolds would be very close to that in Fig. 6b.

The phenomenon of the boundary crisis which results in the annihilation of the chaotic attractor brings us to the problem of the system transient motion: what are main features of the transient motion after the boundary crisis? How the system trajectories leave the region of the phase plane that was formerly occupied by the chaotic attractor? Here we came across the phenomena of *transient*

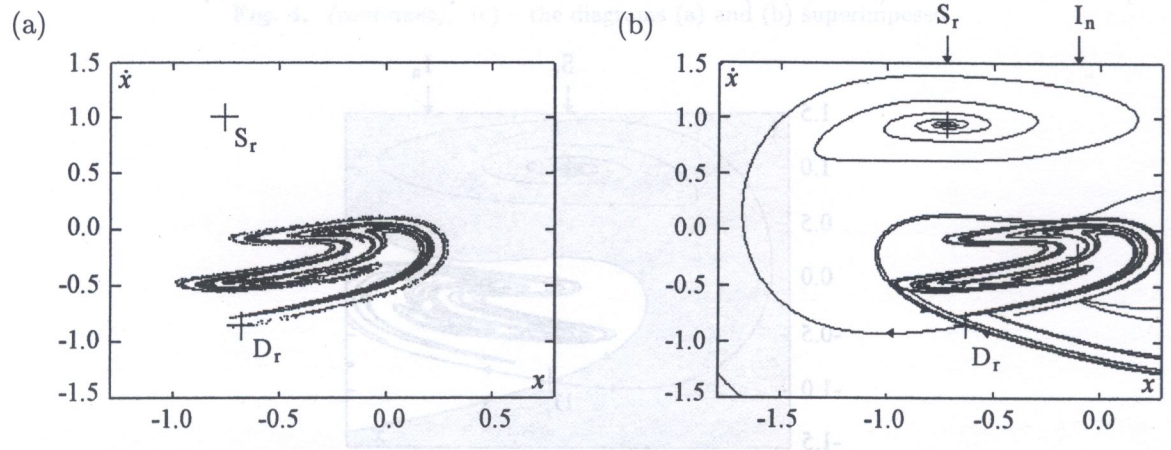

Fig. 6. Boundary crisis of the chaotic attractor: (a) defined as the collision with the saddle D_r; (b) defined as the heteroclinic bifurcation of the saddle D_r and the inverse unstable periodic orbit I_n embedded within the chaotic attractor

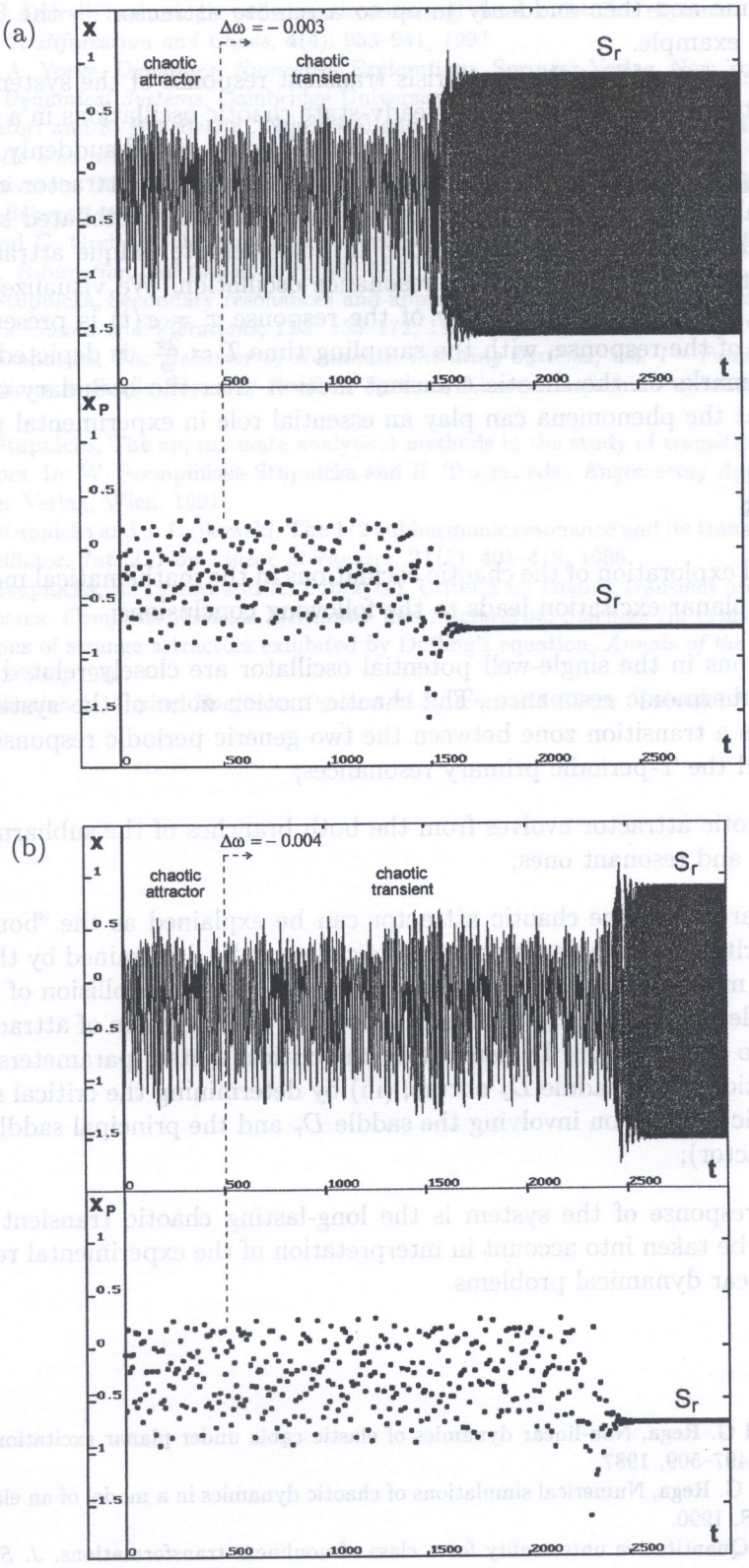

Fig. 7. Two time histories of chaotic transients after crisis of the chaotic attractor, under small-step increments of driving frequency: (a) $\Delta\omega = 0.003$; (b) $\Delta\omega = 0.004$; *upper parts* of both figures represent continuous-time trajectories, *lower parts* denote sampled trajectories (Poincaré maps) with the sampling time $T = \frac{2\pi}{\omega}$

chaos — long lasting, irregular and unpredictable transient motion, that may look like steady-state chaos for a long time and then suddenly jump to a remote attractor — the T-periodic resonant attractor S_r in our example.

Our numerical experiment on the post-crisis transient response of the system was performed in the following way: to the system exhibiting steady-state chaotic oscillations in a close vicinity of the boundary crisis, an increment of the driving frequency $\Delta\omega$ was added suddenly, so that the system was set into the region of the system parameters where the chaotic attractor ceases to exist. Yet, the system still realized the response that looked exactly like the annihilated steady-state chaotic oscillations, until the response suddenly jumped into the remote unique attractor of the system, i.e. the high amplitude T-periodic primary resonance oscillation. We visualize our results in two ways: first the full, continuous time history of the response $x = x(t)$ is presented, and then the stroboscopic image of the response, with the sampling time $T = \frac{2\pi}{\omega}$, is depicted (Figs. 7a and 7b). The preliminary remarks on the chaotic transient motion after the boundary crisis of the chaotic attractor signal that the phenomena can play an essential role in experimental mechanics.

4. Conclusions

The computer aided exploration of the chaotic oscillations in the mathematical model of a suspended elastic cable under planar excitation leads to the following conclusions:

- Chaotic oscillations in the single-well potential oscillator are closely related to the loss of stability of the subharmonic resonance. The chaotic motion zone of the system parameters can be interpreted as a transition zone between the two generic periodic responses: the 2T-periodic subharmonic and the T-periodic primary resonances;
- The full size chaotic attractor evolves from the both branches of the subharmonic resonance — the nonresonant and resonant ones;
- Sudden disappearance of the chaotic attractor can be explained as the "boundary crisis" phenomenon. The critical system parameters of the crisis can be determined by the use of one of the three equivalent methods: (i) by treating the boundary crisis as a collision of the chaotic attractor and the saddle D_r, whose insets define the boundary of the basin of attraction of the chaotic attractor prior to the crisis; (ii) by computing the critical system parameters for which the homoclinic bifurcation of the saddle D_r occurs; (iii) by determining the critical system parameters of the heteroclinic bifurcation involving the saddle D_r and the principal saddle I_n (embedded in the chaotic attractor);
- The post-crisis response of the system is the long-lasting chaotic transient motion; the phenomenon should be taken into account in interpretation of the experimental research carried out in various nonlinear dynamical problems.

References

[1] F. Benedettini and G. Rega, Non-linear dynamics of elastic cable under planar excitation. *Int. J. Non-Linear Mechanics*, **22**(6): 497–509, 1987.

[2] F. Benedettini and G. Rega, Numerical simulations of chaotic dynamics in a model of an elastic cable, *Nonlinear Dynamics*, **1**: 23–38, 1990.

[3] M.J. Feigenbaum, Quantitative universality for a class of nonlinear transformations. *J. Stat. Phys.* **19**: 25–52, 1978.

[4] C. Grebogi, E. Ott and J.A. Yorke, Chaotic attractors in crises. *Phys. Rev. Letters*, **48**: 1507–1510, 1982.

[5] C. Grebogi, E. Ott and J.A. Yorke, Crises, sudden changes in chaotic attractors and transient chaos. *Physica* **D7**: 181–200, 1983.

[6] J. Guckenheimer and P.J. Holmes, *Nonlinear Oscillations, Dynamical Systems and Bifurcations of Vector Fields.* Springer-Verlag, New York, 1983.

[7] Ch. Hayashi, *Nonlinear Oscillations in Physical Systems.* Princeton University Press, Princeton, N.J., 1985.
[8] A.L. Katz and E.H. Dowell, From single well chaos to cross well chaos: a detailed explanation in terms of manifold intersections. *Int. J. Bifurcation and Chaos*, **4**(4): 933–941, 1994.
[9] H.E. Nusse and J.A. Yorke, *Dynamics: Numerical Explorations.* Springer-Verlag, New York, 1994.
[10] E. Ott, *Chaos in Dynamical Systems.* Cambridge University Press, Cambridge, 1993.
[11] G. Rega, A. Salvatori and F. Benedettini, Numerical and geometrical analysis of bifurcations and chaos for an asymmetrical elastic nonlinear oscillator. *Nonlinear Dynamics*, **7**: 249–272, 1995.
[12] G. Rega and A. Salvatori, Bifurcation structure at 1/3 subharmonic resonance in an asymmetric nonlinear elastic oscillator. *Int. J. Bifurcation and Chaos*, **6**(8): 1529–1546, 1996.
[13] J.C. Sommerer and C. Grebogi, Determination of crisis parameters values by direct observation of manifold tangencies. *Int. J. Bifurcation and Chaos*, **2**(2): 383–396, 1992.
[14] W. Szemplińska-Stupnicka, Secondary resonances and approximate models of routes to chaotic motions in non-linear oscillators. *J. Sound and Vibrations*, **113**: 155–172, 1987.
[15] W. Szemplińska-Stupnicka, *The Behavior of Nonlinear Vibrating Systems; vol. I – Fundamental Concepts and Methods: Applications to Single-Degree-of-Freedom Systems*, Kluwer Academic Publishers, Dordrecht–Boston–London, 1990.
[16] W. Szemplińska-Stupnicka, The approximate analytical methods in the study of transition to chaotic motion in nonlinear oscillators. In: W. Szemplińska-Stupnicka and H. Troger, eds., *Engineering Applications of Dynamics of Chaos,* Springer Verlag, Wien, 1991.
[17] W. Szemplińska-Stupnicka and J. Bajkowski, The 1/2 subharmonic resonance and its transition to chaotic motion in a nonlinear oscillator. *Int. J. Non-Linear Mechanics*, **21**(5): 401–419, 1986.
[18] W. Szemplińska-Stupnicka, E. Tyrkiel and A. Zubrzycki, Criteria for chaotic transient oscillations in a model of driven buckled beams. *Computer Assisted Mechanics and Engineering Sciences* (in print), 1999.
[19] Y. Ueda, Explosions of strange attractors exhibited by Duffing's equation. *Annals of the New York Academy of Sciences,* **357**: 422–433, 1980.
[20] S. Wiggins, *Introduction to Applied Nonlinear Dynamical Systems and Chaos.* Springer-Verlag, New York, 1990.